Noise-induced Effects in Nonlinear Relaxation of Condensed Matter Systems

B. Spagnolo[a,b,c,*], D. Valenti[a], C. Guarcello[a,c], A. Carollo[a], D. Persano Adorno[a], S. Spezia[a], N. Pizzolato[a], B. Di Paola[d]

[a] *Dipartimento di Fisica e Chimica, Group of Interdisciplinary Theoretical Physics, Università di Palermo and CNISM-Unità di Palermo, Viale delle Scienze, edificio 18, I-90128 Palermo, Italy*

[b] *Istituto Nazionale di Fisica Nucleare, Sezione di Catania, Via Santa Sofia 64, I-95123 Catania, Italy*

[c] *Radiophysics Department, Lobachevsky State University, Gagarin ave.23, 603950 Nizhni Novgorod, Russia*

[d] *Dipartimento di Matematica e Informatica, via Archirafi, 34, I-90123 Palermo (Italia)*

Abstract

Noise-induced phenomena characterise the nonlinear relaxation of nonequilibrium physical systems towards equilibrium states. Often, this relaxation process proceeds through metastable states and the noise can give rise to resonant phenomena with an enhancement of lifetime of these states or some coherent state of the condensed matter system considered. Specifically three noise induced phenomena, namely the noise enhanced stability, the stochastic resonant activation and the noise-induced coherence of electron spin will be reviewed in the nonlinear relaxation dynamics of three different systems of condensed matter: (i) a long-overlap Josephson junction (JJ) subject to thermal fluctuations and non-Gaussian, Lévy distributed, noise sources; (ii) a graphene-based Josephson junction subject to thermal fluctuations; (iii) electrons in a n-type GaAs crystal driven by a fluctuating electric field. In the first system, we focus on the switching events from the superconducting metastable state to the resistive state, by solving the perturbed stochastic sine-Gordon equation. Nonmonotonic behaviours of the mean switching time versus the noise intensity, frequency of the external driving, and length of the junction are obtained. Moreover, the influence of the noise induced solitons

*URL: https://sites.google.com/site/itpgunipa/home

*corresponding author (E-mail: bernardo.spagnolo@unipa.it)

on the mean switching time behaviour is shown. In the second system, noise induced phenomena are observed, such as noise enhanced stability (NES) and stochastic resonant activation (SRA). In the third system, the spin polarised transport in GaAs is explored in two different scenarios, i.e. in the presence of Gaussian correlated fluctuations or symmetric dichotomous noise. Numerical results indicate an increase of the electron spin lifetime by rising the strength of the random fluctuating component. Furthermore, our findings for the electron spin depolarization time as a function of the noise correlation time point out (i) a non-monotonic behaviour with a maximum in the case of Gaussian correlated fluctuations, (ii) an increase up to a plateau in the case of dichotomous noise. The noise enhances the coherence of the spin relaxation process.

Keywords: Noise processes and phenomena; Josephson junction; Stochastic analysis methods; Noise enhanced stability; Resonant activation; Spin polarised transport in semiconductors; Monte Carlo methods
PACS: 72.70.+m, 85.25.Cp, 05.10.Gg, 81.05.ue, 74.40.-n, 72.25.Dc, 05.10.Gc

1. Introduction

The nonlinear relaxation process in many condensed matter systems proceeds through metastable states, giving rise to nonmonotonic behaviors of the lifetime of the metastable state as a function of the noise intensity or some external driving frequency. Moreover, the noise can enhance the electron spin lifetime in semiconductor crystals for an initial metastable state with all spin aligned. Metastability, in fact, is a generic feature of many nonlinear systems, and the problem of the lifetime of metastable states involves fundamental aspects of nonequilibrium statistical mechanics. Nonequilibrium systems are usually open systems which strongly interact with the environment and this interaction can be modeled as a noise source. The investigation of noise induced phenomena in far from equilibrium systems is one of the approaches used to understand the behavior of condensed matter complex systems.

In this paper we shortly review three noise induced effects in condensed matter systems, namely the noise enhanced stability and the stochastic resonant activation in JJs and the noise-induced coherence of electron spin in a spintronic system. Specifically we will consider the nonlinear relaxation process of long and short JJs and spin transport in GaAs. Moreover, new results concerning the out of equilibrium dynamics of graphene-based JJ and

the spin depolarisation process are presented.

1.1. Long JJ

A Josephson junction (JJ) is a device realised by sandwiching two superconducting plates on a interlayer of non-superconducting material. In this mesoscopic device, macroscopic quantities as voltage and current are directly related to a microscopic order parameter φ, representing the phase difference between the wavefunctions of charge carriers in the two superconducting electrodes. In fact, great attention has been paid to JJs as superconducting quantum bits [1]-[4], nanoscale superconducting quantum interference devices for detecting weak flux changes [5, 6], and threshold noise detectors [7]-[10]. Moreover JJs are typical out of equilibrium systems characterised by tilted or switching periodic potentials [11, 12], and the effects both of thermal and non-thermal noise sources on the transient dynamics of JJs have recently attracted considerable interest [13]-[23]. In the last decade, theoretical progress has allowed to calculate the entire probability distribution of the noise signal and its cumulants, performing a *full counting statistics* of the current fluctuations [14]. Moreover, the presence of non-Gaussian noise signals has been observed experimentally in several systems [13, 17], [24]-[27]. As an example in a wireless ad hoc network with a Poisson field of co-channel users, the noise has been well modelled by an α-stable distribution [27]. Non-equilibrated heat reservoir can be looked as a non-Gaussian noise sources [24]-[26]. In particular, the effects of non-Gaussian noise on the average escape time from the superconducting metastable state of a biased junction coupled with nonequilibrium current fluctuations, has been experimentally examined [13, 17].

Recently, the characterisation of JJs as detectors, based on the statistics of the escape times, has been proposed [7]-[10], [19]-[23]. Specifically, the statistical analysis of the switching from the metastable superconducting state to the resistive running state of the JJ has been proposed to detect weak periodic signals embedded in a noise environment [9, 10]. Moreover, the rate of escape from one of the metastable wells of the tilted washboard potential of a JJ encodes information about the non-Gaussian noise present in the input signal [7, 8], [19]-[23].

Here, the theoretical results for nonmonotonic behaviours of the mean switching time (MST) in a long JJ as a function of the noise intensity, frequency of the external driving current, and junction length are shown and analysed. Specifically, we try to understand how non-Gaussian noise sources

affect the switching times in long JJs. The model and the results are presented in Section 2.

1.2. Graphene JJ

The Josephson effect came to light also in a particular kind of JJs, in which the interlayer is a graphene sheet. The resistance of the graphene to the surface oxidation makes this material a good candidate for the realisation of high quality junctions. These devices seem good candidates for the realisation of gate-tunable phase qubits [28, 29]. The current-phase relation (CΦR) for superconductor - graphene - superconductor (SGS) device composed by two electrodes "suspended" over a graphene substrate (see Fig. 6a), was deeply studied in Refs. [30, 31]. Moreover, noise signatures in the behaviour of graphene junctions characterise many experimental and theoretical works [28], [32]-[36]. Here we analyse the transient dynamics and the escape process from metastable states in a SGS device. The model and the results are discussed in Section 3.

1.3. Spin polarised transport

In recent years, diffusion in heterostructures [37] and transport in semiconductors [38] have been increasingly investigated. In particular, the interest in developing spin-based devices gave rise to a huge number of investigations on spin phenomena in semiconductors, with the aim to control the electron spin polarisation by means of electric currents or gate voltages [39]-[44]. Nevertheless, a drawback of the use of the electron spin is the fact that the magnetic polarization relaxes over time during the transport because of spin-orbit interactions or scattering events.

Since the spin lifetime could be too short to enable the entire execution of the necessary spin manipulations, the investigation of the spin relaxation processes in spintronic device design is a crucial point [40, 41]. In the last decades, great interest has been oriented towards the noise-induced phenomena in nonlinear complex systems, such as conduction electrons inside semiconductor structures [45]. Noise enhanced stability phenomenon [46]-[48] in the electron transport inside GaAs bulks, caused by the addition of external fluctuations to the driving oscillating electric field, has been reported in Refs. [49]-[51]. Recently, in semiconductor quantum wells and quantum wires the possibility of exploiting random Rashba spin-orbit interaction to generate spin currents has been found [52]. Specifically, Monte Carlo simulations have evidenced that the spatial variation of the Rashba electric field

along the quantum wire length yields the spatial spin depolarization process random, non-monotonic and chaotic [53]. Previous studies of the electron spin decoherence process in GaAs crystals have revealed that a Gaussian random contribution added to the static driving field can change both the spin depolarization time and length [54, 55]. Moreover, recently it has been found that the electron spin lifetime can be changed also when dichotomous random fluctuations are externally added to the driving electric field [56]. In all cases, the external noise can have opposite effects on the electron spin depolarization process, critically depending on the strength of both the applied voltage and the external noise, as well as on the fluctuation correlation time.

In Section 4, the effects on the electron spin depolarization of two different fluctuating contributions, namely a Gaussian correlated noise and a symmetric dichotomous one, to the driving electric field in n-doped GaAs crystals, are shown. The analysis is performed by varying the amplitude of the electric driving field, the noise correlation times and the external fluctuation amplitude, discussing the possibility of "tuning" the rate of the spin relaxation process.

Finally, in Section 5 we have drawn the conclusions.

2. Long JJ - The sine-Gordon model

The I-V characteristics of a long JJ is directly related to the transient dynamics of the order parameter φ, that is the phase difference across the junction. The φ evolution is described by the well-known sine-Gordon (SG) equation, shown below in the so-called perturbed form, namely including bias and fluctuating currents $i_b(x,t)$ and $i_f(x,t)$, respectively, and a damping term [57, 58]

$$\beta_{_{SG}}\varphi_{tt}(x,t) - \varphi_{xx}(x,t) + \sin(\varphi(x,t)) = i_b(x,t) + i_f(x,t) - \varphi_t(x,t). \qquad (1)$$

The subscripts of φ represent partial derivatives in the indicated variables. In Eq. (1) the variables x and t are normalised to the Josephson penetration length λ_J and the characteristic JJ frequency ω_c, respectively. The coefficient $\beta_{_{SG}}$ is related to the details of the junction, according to $\beta_{_{SG}} = \omega_c RC$, where R and C are the effective normal resistance and capacitance of the device. The $\sin(\varphi)$ term is the supercurrent. All the current terms in Eq. (1) are normalised to the JJ critical current I_c. The presence of an external magnetic

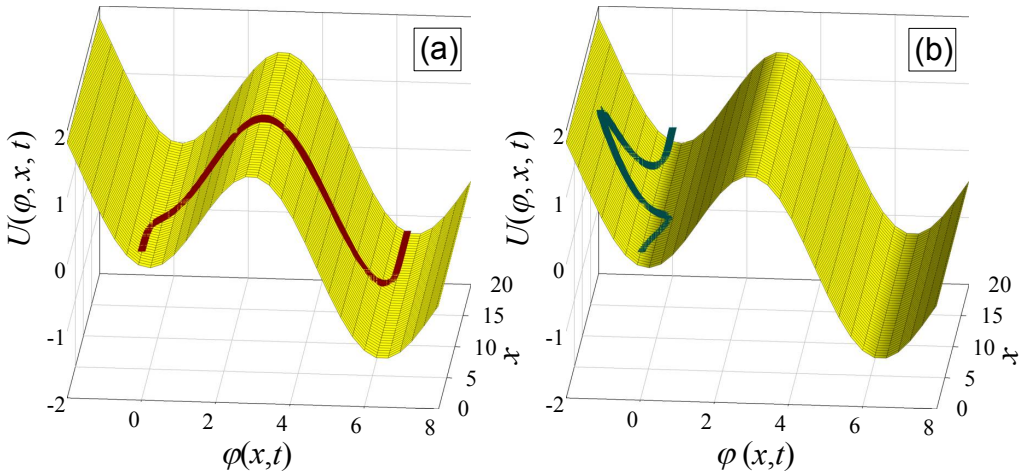

Figure 1: (Color online) (a) Tilted washboard potential with a soliton located between two neighbouring valleys. (b) Tilted washboard potential with a breather.

field is taken into account in the boundary conditions

$$\varphi_x(0,t) = \varphi_x(L,t) = \Gamma, \tag{2}$$

where Γ is the normalised magnetic field and L is the junction length in unit of λ_J. The analysis is carried out in absence of applied magnetic field, i.e $\Gamma = 0$. Usually, the dynamics of a long JJ can be described as that of a phase *string* of length L, whose elements are named *cells*. The string is placed on a tilted potential, the *washboard potential* (WP), which is characterised by a sequence of wells (see Fig. 1) and it is expressed by

$$U(\varphi, x, t) = 1 - \cos(\varphi(x,t)) - i_b(x,t)\,\varphi(x,t). \tag{3}$$

The junction remains superconductive until the string entirely lies within a potential well, otherwise it undergoes a resistive behaviour. The SG equation admits various traveling wave solutions, that is solitons, antisolitons and breathers. Specifically, the soliton stochastic dynamics in JJs has been largely investigated [59]-[64]. A SG soliton is a 2π step in φ, corresponding to a string placed between two neighbouring valleys of the WP, as it is shown in panel (a) of Fig. 1. In the unperturbed SG model, the analytic expression of a soliton solution is

$$\varphi(x-ut) = 4\arctan\left\{\exp\left[\pm\frac{(x-ut)}{\sqrt{1-u^2}}\right]\right\}, \tag{4}$$

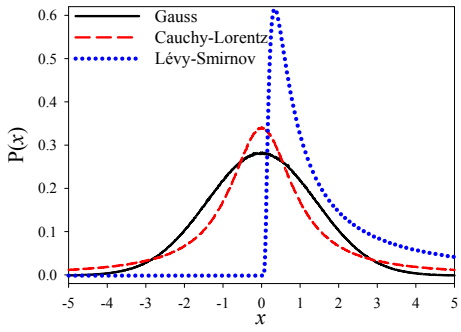

Figure 2: (Color online) Probability density functions for Gaussian (G), Cauchy-Lorentz (CL) and Lévy-Smirnov (LS) distributions.

Distr.	P(x)		$S_\alpha(\sigma,\beta,\mu)$
G	$\frac{1}{\sqrt{2\pi}\sigma} e^{-\frac{(x-\mu)^2}{2\sigma^2}}$	$x \in \mathbb{R}$	$S_2(\sigma,0,\mu)$
CL	$\frac{\sigma/\pi}{\sigma^2+(x-\mu)^2}$	$x \in \mathbb{R}$	$S_1(\sigma,0,\mu)$
LS	$\sqrt{\frac{\sigma}{2\pi}} \frac{e^{-\frac{\sigma}{2(x-\mu)}}}{(x-\mu)^{3/2}}$	$x \geq \mu$	$S_{\frac{1}{2}}(\sigma,1,\mu)$

Table 1: Closed form of Gaussian (G), Cauchy-Lorentz (CL) and Lévy-Smirnov (LS) distributions and characteristic values of parameters.

where u is the Swihart velocity and the sign $\pm$ distinguishes between a soliton and an antisoliton. A breather is a soliton-antisoliton bounded couple oscillating in an internal frame with a proper frequency. A string excited by a breather is shown in panel (b) of Fig. 1. The bias current used in our model is

$$i_b(x,t) = i_0(x) + A\,\sin(\omega t), \tag{5}$$

and it represents the inclination of the potential, so that $i_b(x,t) > 1$ means a WP so tilted that its "maxima and minima" structure vanishes, corresponding to the absence of metastable states. Therefore, the i_b value is also directly related to the height of the right and left potential barriers that the phase string has to overcome to switch to the resistive state. In this work we set $A = 0.7$, $i_0(x) = i_0$, that is constant values, and the driving frequency ω ranging in the interval $[10^{-2}, 10^2]$. Other more refined models use spatially dependent bias current distributions, which increase considerably close to the junction ends [22, 23].

2.1. Long JJ - The Lévy statistics

In this section, we discuss several cases [65] in which non-Gaussian stable statistics, connected to the generalised Central Limit Theorem [66]-[72], is used to model experimental data characterized by asymmetric distributions with heavy tails. The α-stable (or Lévy) distributions can be indicated using the symbol $S_\alpha(\sigma,\beta,\mu)$. This notation needs four parameters: an *asymmetry*

parameter β with $|\beta| \leq 1$, a *stability index* (or characteristic exponent) $\alpha \in]0, 2]$ which rules how the distribution tails go to zero and two real numbers $\sigma > 0$ and μ which determine the profile of the distribution and are named *shape parameters*. In particular, setting $\beta = 0$ ($\beta \neq 0$) the distribution is a symmetric (asymmetric). For $\alpha < 2$ the asymptotic behaviour is described by a power law, while a Gaussian distribution results from $\alpha = 2$ and $\beta = 0$. Setting $\sigma = 1$ and $\mu = 0$, the stable distributions are named *standard*. Only few Lévy distributions have a probability density function known in explicit form, as shown in Table (1). The abbreviations for the peculiar distributions used in the rest of this work are listed in Table (1). The Gaussian (G) and Cauchy-Lorentz (CL) distributions have $\beta = 0$ and are symmetrical with respect to $x = \mu$, while the Lévy-Smirnov (LS) distributions normal and reflected are skewed to the right ($\beta = 1$) or left ($\beta = -1$) side, respectively. The distributions of Table (1) are presented in Fig. 2. The asymmetry of the LS distribution, with a narrow peak located at a positive value of x followed by a heavy tail, is evident. In comparison with the Gaussian one, the CL distribution has higher tails and a central part of the distribution more concentrated around the mean value. For short times, the random values distributed according to the CL statistics define trajectories characterised by *limited space displacement*. The CL statistics is characterised, around the mean value, by a narrower distribution with respect to the Gaussian one. However, for longer times heavy tails result in events with large values of x, whose probability densities are not negligible. Using CL and LS statistics rare events are taken into account, because of the fat tails of these distributions. These events represent the so-called Lévy flights. In this work, to simulate Lévy noise sources we use the algorithm proposed by Weron [73] to implement the Chambers method [74]

2.2. Long JJ - results and discussions

We computationally study the mean switching time (MST) of an overdamped JJ ($\beta_{_{SG}} = 0.01$). Here, no absorbing barriers are considered, and the MST is calculated as nonlinear relaxation time (NLRT) [48], according to definition given in Refs. [75]-[79]. In order to obtain the mean values of the switching times we perform a suitable number ($N = 5000$) of numerical realisations. As initial condition we set the string at the bottom of the first WP valley, that is $\varphi_0 = \arcsin(i_b(x, 0)) = \arcsin(i_0)$. The calculations are performed for the three noise statistics given in the previous section, obtaining

the behaviour of the MST τ in the presence of different sources of Lévy noise.

MST vs JJ length L − We begin to study the MST values varying the JJ length L in the range $[0, 20]$. The results obtained setting $i_0 = 0.5$ and $\omega = 0.4$ are shown in Fig. 3, emphasising the three different noise sources used, G (panel a), CL (panel b) and LS (panel c). The amplitude of the oscillating driving signal is set at $A = 0.7$, to obtain during the oscillation (see Eq. (5)) both $i_b > 1$ (absence of metastable states) and $i_b < 0$ (positive slope). The results shown in Fig. 3 clearly indicate an overall reduction of the MST values as the noise amplitude increases, since the higher the γ value is the faster the cells are pushed out from the initial metastable state. The curves obtained using Gaussian noise sources (panel a of Fig. 3) show the occurrence of two different dynamical regimes. Up to a critical length $[23, 80]$, an initial monotonic increasing behaviour characterises the values of τ, but exceeding this critical length a constant MST plateau is established. The different mechanisms ruling these two regimes are clearly explained in Fig. 4. For a short junction (see panel (a) of Fig. 4 obtained for $L = 2$) the string tends to move between the WP valleys as a whole, because the connection among cells is so strong that the soliton formation is forbidden. In the short junction regime, an increase in the number of cells makes more difficult the motion of the whole string during the transition process, causing the MST to raise for short lengths. For junction lengths greater than the critical value it is evident a saturation effect. The MST reaches an almost constant value and switching events are driven by the solitons, as shown in panel (b) of Fig. 4, obtained for $L = 10$. Panels (b) and (c) of Fig. 3 show MST curves obtained in the presence of CL and LS noise sources, respectively. These behaviors appear quite different with respect to those obtained using a Gaussian noise source. The MST curves are strongly affected by Lévy flights that favour jumps between different potential valleys and soliton formation (see Fig. 4, containing rapid and sudden phase variations). Specifically, for CL noise the saturation effect gives rise to a value of MST lower than that observed with the Gaussian thermal fluctuations. This is due to the peculiarity of the fat tails of PDF for CL noise. Furthermore, LS noise drives the phase string out of the potential well very quickly, due to the greater diffusive power of this noise source. The curves of Fig. 4, obtained using a CL noise source, show peaks associated with the generation of Lévy flights. These noise induced fluctuations influence the switching events and the soliton formation. These graphs also clearly display the creation of another "structure", known

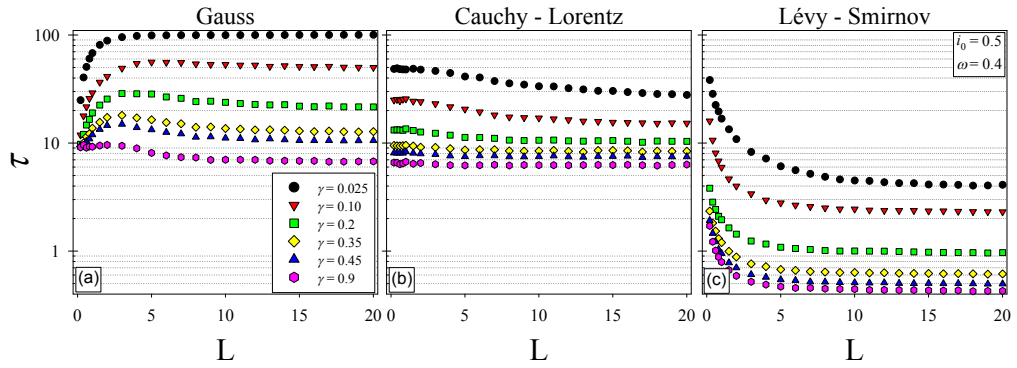

Figure 3: (Color online) MST τ as a function of the length L of the junction, for different noise intensities $\gamma = \{0.025, 0.10, 0.2, 0.35, 0.45, 0.9\}$, setting $i_b = 0.5$, $\omega = 0.4$ and using different noise source statistics, that is Gaussian (panel a), Cauchy-Lorentz (panel b) and Lévy-Smirnov (panel c). The legend shown in panel (a) refers also to other panels.

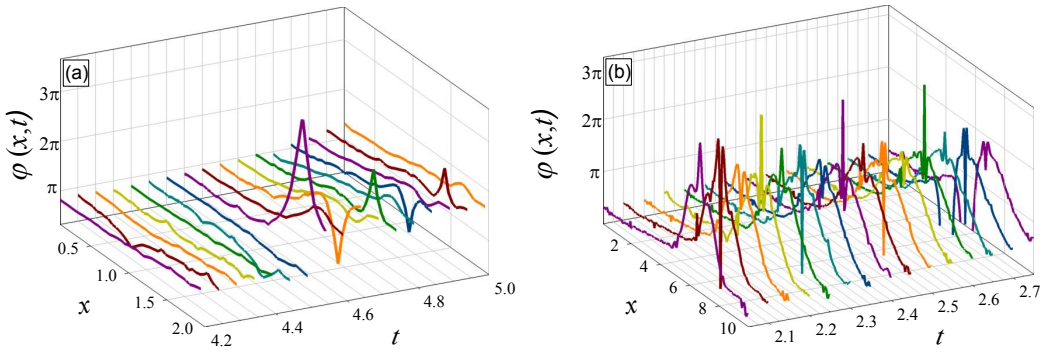

Figure 4: (Color online) String dynamics during the switching towards the resistive state: for a JJ of length $L = 2$ (panel a) and $L = 10$ (panel b). All graphs were obtained for $\omega = 0.4$, $\gamma = 0.2$ and CL noise source. The curves show the characteristic Lévy flights of the CL statistics.

as *breather*. This is a well-known localised solution of the SG equation, consisting of a soliton-antisoliton pair oscillating with an internal "breathing" frequency. Here, we name this particular solution of the SG equation *noise-induced breather*.

MST vs driving frequency ω – In this subsection we study the MST τ behaviour as a function of the driving frequency $\omega \in [10^{-2} - 10]$, setting $L = 6$ and $\gamma = 0.1$, varying the bias value $i_0 = \{0.5, 0.9\}$ and the statistics of the noise sources. The data obtained are shown in panel (a) of Fig. 5. The

junctions are long enough to give rise to solitons along the string. All graphs clearly show the presence of *resonant activation* (RA) [48], [81]-[91], specifically *stochastic resonance activation*, a noise induced phenomenon, whose signature is the appearance of a minimum in the curve of MST *vs* ω [10, 23]. The RA is a phenomenon sufficiently robust to be found also in the presence of Lévy noise sources [92, 22, 23]. Particle escape from a potential well occurs, in average, when the potential barrier oscillates on a time-scale characteristic of the particle escape itself. Since the resonant frequency is close to the inverse of the average escape time in the minimum, which is the mean escape time over the potential barrier in the lower configuration, *stochastic resonant activation* occurs [10, 23, 93]. This is a phenomenon different from the *dynamic resonant activation*, which occurs when the driving frequency matches the natural frequency of the system, that is the plasma frequency [94]-[96]. By increasing the driving frequency, at low noise intensities, a trapping phenomenon occurs. A threshold frequency ω_{thr} exists such that for $\omega > \omega_{thr}$ the phase string is trapped within a region between two adjacent minima of the potential profile. In other words, the string can not advance from the potential well to the next one during one period T_0 of the oscillating current $A\sin(\omega t)$. Therefore, the MST diverges in the limit $\gamma \to 0$. The value of the threshold frequency increases with increasing bias current and/or maximal current across the junction [47, 48].

MST vs noise amplitude γ − Here we explore the behaviour of the MST τ, varying the noise amplitude γ in the range $[5 \cdot 10^{-4}, 2 \cdot 10^{2}]$. The results are shown in panel (b) of Fig. 5 for $L = 6$ and $\omega = 0.9$. Two different inclinations of the WP are taken into account, imposing $i_0 = \{0.5, 0.9\}$, and considering G, CL and LS noise statistics. For $\gamma \to 0$, all curves converge to the deterministic lifetime of the superconducting state. For weak noise intensities and intermediate slope of the WP, trapping phenomena occur, i.e. $\tau \to T_{max}$. Increasing γ, the MST curves exhibit an effect of *noise enhanced stability* (NES), a noise induced phenomenon observed in different physical systems [46]-[48], [97]-[117], consisting in a nonmonotonic behaviour of τ vs γ with the appearance of a maximum. The curves calculated for G noise sources and high slope, i.e. $i_b = 0.9$, show an evident double maxima NES effect [23]. The maximum for high noise amplitudes is related to the possibility that the phase string returns into the initial valley after a first escape event. This second peak tends to vanish in CL curves, due to the action of the CL Lévy flights. The differences between the first NES maximum obtained using a

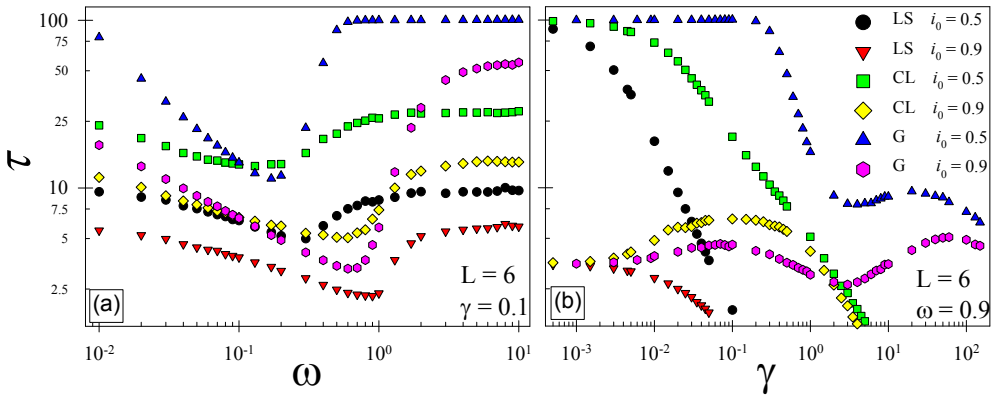

Figure 5: (Color online) (a) MST τ as a function of the driving frequency ω, setting $\gamma = 0.1$. (b) MST τ as a function of the noise amplitude γ, setting $\omega = 0.9$. The legend in panel (b) refers also to panel (a). For both panels, $L = 6$, $i_0 = \{0.5, 0.9\}$ and G, CL and LS noise source statistics are used.

G noise and that obtained by a CL noise source can be ascribed to the *limited space displacement* that characterises the CL distribution for short time scales and low noise intensities. The LS τ values tend to rapidly decrease as γ increases, because very intense Lévy flights tend to rapidly push the cells out of the potential minimum.

3. Graphene JJ

For a short ballistic SGS junction, in the low temperature limit, the expressions of the supercurrent $i_\varphi(t)$ and washboard potential (WP) $U(\varphi)$ were obtained in Refs. [30, 31]. A non-sinusoidal phase-dependence of $i_\varphi(t)$ and $U(\varphi)$ is found, unlike the conventional junctions, that is ruled by the well-known d.c. Josephson relation. Noise signatures in the behaviour of graphene junctions characterise many experimental and theoretical works [28], [32]-[36]. In this paper we explore the switching dynamics of an underdamped SGS junction in the presence of an external noise source. The analysis is performed by varying the amplitude i_b and frequency ω of the applied bias current, and the intensity γ of the noise signal. We compare the results obtained for a graphene-based JJ with the analogous ones calculated considering a conventional JJ. Our work sheds light on the transient dynamics and the escape events from the metastable states of the WP of a graphene-based

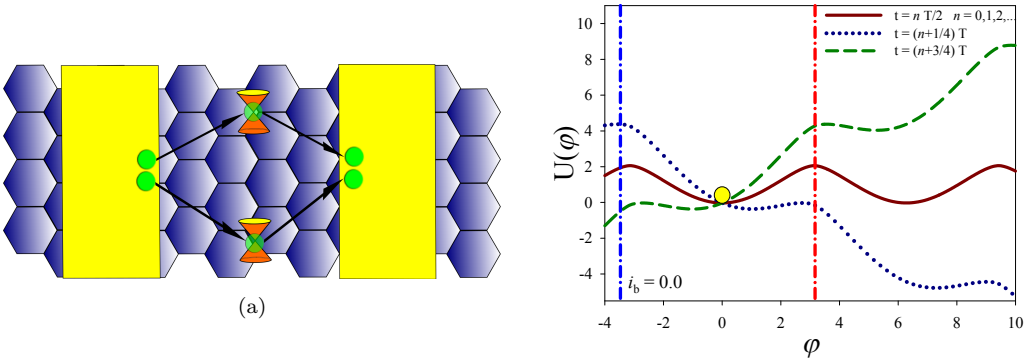

(a) (b)

Figure 6: (a) (Color online) Schematic view of a suspended SGS junction structure. (b) Washboard potential $U(\varphi)$ as a function of the phase φ for a graphene-based JJ with $i_b = 0$. Three different configurations are shown, corresponding to different values of $\sin(\omega t)$ (see Eqs. (6) and (5)), namely zero (dark red, solid line), maximum (green, dashed line) and minimum (dark blue, dotted line) slopes of the potential profile. Red and blue dashed-dotted lines represent the right and left absorbing barriers, respectively. In the legend, T is the oscillation period of the potential.

junction (see Fig. 6bb), provided that the proper CΦR [30] is considered.

3.1. Graphene JJ - The model

The time evolution of the order parameter φ for a short JJ is ruled by the RCSJ model [57]. The equation for the motion of φ is

$$\varphi_{tt}(t) + \beta_J \varphi_t(t) = i_b(t) - i_\varphi(t) + i_f(t) \tag{6}$$

where β_J is the damping parameter calculated according to the Johnson approach [57]. The time variable in Eq. (6) is normalised to the inverse of the JJ plasma frequency. The current terms $i_b(t)$, $i_\varphi(t)$ and $i_f(t)$ are the bias current, the supercurrent and the fluctuating current, respectively, normalised to the JJ critical current value. The bias current is given by

$$i_b(t) = i_0 + A\sin(\omega t), \tag{7}$$

where i_0 is the initial value, $A = 0.7$ and ω are the amplitude and frequency of the oscillating part.

For a SGS junction, the deviation from the conventional sinusoidal behaviour of the supercurrent was analytically obtained by Titov and Beenakker [30].

In the limit of small temperature, $T \to 0$, they obtained the supercurrent and its critical value for a short ballistic junction

$$i_\varphi(\varphi(t)) = \frac{I(\varphi)}{I_c} = \frac{2}{1.33}\cos\left(\frac{\varphi}{2}\right)\tanh^{-1}\left[\sin\left(\frac{\varphi}{2}\right)\right] \quad (8)$$

$$I_c = 1.33\frac{e\Delta_0}{\hbar}\frac{W}{\pi L}. \quad (9)$$

Using the previous Josephson current, Lambert *et al.* [31] derived the following expression of the washboard-like potential

$$U(\varphi,t) = - E_{J0}\Bigg\{ - \frac{2}{1.33}\Bigg\{2\sin\left(\frac{\varphi}{2}\right)\tanh^{-1}\left[\sin\left(\frac{\varphi}{2}\right)\right] + + \ln\left[1-\sin^2\left(\frac{\varphi}{2}\right)\right]\Bigg\} + i_b(t)\varphi\Bigg\}, \quad (10)$$

where $E_{J0} = \Phi_0 i_c/2\pi$ is the Josephson coupling energy and $\Phi_0 = h/2e$ is the magnetic flux quantum. As a conventional WP, the slope is represented by the bias current and the position of the phase particle along the potential profile defines the working regime, superconducting or resistive, of the device. The graphene WP is shown in Fig. 6b for three different slopes (zero, maximum and minimum) with $i_b = 0$. The mean escape time τ is calculated as mean first passage time (MFPT). Two absorbing barriers are placed in correspondence of the WP maxima closer to the initial minimum, chosen as initial condition (see the dashed-dotted lines of Fig. 6b).

The thermal fluctuations of the current i_f are modelled by a Gaussian noise source with the well-known statistical properties

$$\langle i_f(t)\rangle = 0, \qquad \langle i_f(t) i_f(t+\tau)\rangle = 2\gamma(T)\delta(\tau) \quad (11)$$

In Eq. (11), the dimensionless amplitude is $\gamma(T) = kT/E_{J0}$ and T is the temperature.

3.2. Graphene JJ - Results

The analysis of the MFPT τ as a function of ω and γ is developed mainly varying the slope of the WP, that is using different values of the initial bias current i_0. The heights $\Delta U^\pm$ of the right and left potential barriers strictly follow the modifications of the slope of the potential. In particular, $\Delta U^\pm \to 0$ when $i_b \to \pm 1$.

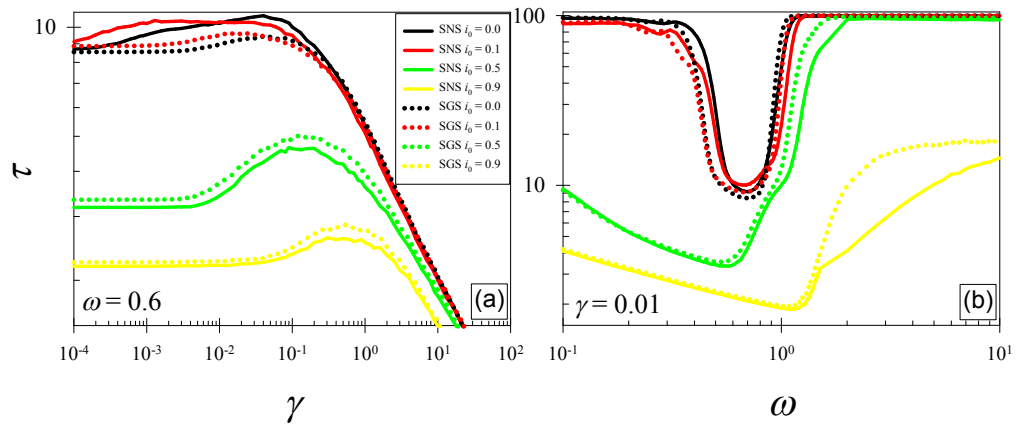

Figure 7: (Color online) (a) MFPT as a function of γ, with fixed frequency $\omega = 0.6$. (b) MFPT as a function of ω, with fixed noise intensity $\gamma = 0.01$. In both panels different initial values of the bias current are used: $i_0 = 0.0, 0.1, 0.5, 0.9$, and $A = 0.7$. Solid and dotted lines represent results for a conventional JJ (SNS in the legend) and a SGS junction, respectively. Legend in panel (a) refers to both panels.

Therefore, the transient dynamics of the phase particle is strongly influenced by the values assumed by the bias current. For this reason we analyse the transient dynamics of a short graphene-based junction, using different initial values of the bias current (WP slope): $i_0 = 0.0$ (zero slope), 0.1 (small slope), 0.5 (intermediate slope) and 0.9 (high slope). The study is developed for both a graphene-based and a normal JJ.

The results are shown in Fig. 7. Panel (a) of this figure contains MFPT curves as a function of the amplitude of the Gaussian noise signal γ, with fixed frequency $\omega = 0.6$. All curves show signature of the NES effect, but the characteristic of the NES maxima depends from the initial values of the bias current i_0.

For very low initial values of the bias current slope, the value of the maximum of τ (see Fig. 7a) for a graphene-based junction, compared to that obtained for a normal JJ (SNS), is clearly smaller. Viceversa, for intermediate and high slopes, the maximum of τ for a SGS increases. These peculiarities should be ascribed to the different potential profile "felt" by the phase particle during its nonlinear relaxation motion.

The values of τas a function of the driving frequency ω, with a fixed noise intensity $\gamma = 0.1$, are shown in panel (b) of Fig. 7. The RA effect is clearly

visible in all the curves, with differences again related to the slopes of the potential profile. A comparison with the results obtained for a SNS, shows a shift of all curves towards lower values of the frequency ω, again due to the peculiarities of the WP in a SGS junction.

4. Electron spin decay modelling

In n-type III-V semiconductors, under nondegenerate regime, the dominant electron spin relaxation process is the D'yakonov-Perel (DP) mechanism [118, 119]. The spin-orbit interaction couples the spin of conduction electrons to the carrier momentum, randomized by interactions with phonons, impurities and other electrons. The spin-orbit coupling produces the spin precession, while momentum scattering makes the precession randomly varying, both in orientation and magnitude [40, 41]. The part of the Hamiltonian of a single electron in the conduction band which takes into account the spin-orbit coupling is given by

$$H_{SO} = \frac{\hbar}{2}\vec{\sigma} \cdot \vec{\Omega}(\vec{k}). \tag{12}$$

H_{SO} accounts for the energy of an electron spin precessing with angular frequency $\vec{\Omega}$ around an effective magnetic field given by

$$\vec{B} = \hbar\vec{\Omega}(\vec{k})/\mu_B g \tag{13}$$

where μ_B is the Bohr magneton and g is the electron spin g-factor. $\vec{\Omega}$ depends on the orientation of the electron momentum vector with respect to the crystal axes. Near the bottom of the Γ-valley the precession frequency is

$$\vec{\Omega}_\Gamma = \frac{\beta_\Gamma}{\hbar}[k_x(k_y^2 - k_z^2)\hat{x} + k_y(k_z^2 - k_x^2)\hat{y} + k_z(k_x^2 - k_y^2)\hat{z}] \tag{14}$$

Near the bottom of the L-valleys, located along the [111] direction in the crystallographic axes [121], the precession vector can be written as

$$\vec{\Omega}_L = \frac{\beta_L}{\sqrt{3}}[(k_y - k_z)\hat{x} + (k_z - k_x)\hat{y} + (k_x - k_y)\hat{z}] \tag{15}$$

In equations (14)-(15), k_i $(i = x, y, z)$ are the components of the electron wave vector, β_Γ and β_L are the spin-orbit interaction coefficients. Here, we set β_Γ= 23.9 eV $\cdot$Å^3, as in Ref. [120] and β_L=0.26 eV Å$\cdot 2/\hbar$, as theoretically estimated

in Ref. [122]. As the quantum-mechanical description of the electron spin evolution is equivalent to that of a classical momentum $\vec{S}$ experiencing the magnetic field $\vec{B}$, we describe the electron spin dynamics by means of the classical equation of precession motion

$$\frac{d\vec{S}}{dt} = \vec{\Omega} \times \vec{S}. \tag{16}$$

The DP mechanism works between two collision events and randomizes spin phases since electrons precess with different frequencies depending on their momenta. In fact, the direction of the precession axis and the effective magnetic field $\vec{B}$ changes randomly and in a trajectory-dependent manner. This makes the spin precession frequencies $\vec{\Omega}$ and their directions varying in an inhomogeneous manner within the electron spin ensemble. This spatial variation, known as *inhomogeneous broadening*, can be quantified by the average squared precession frequency $\langle \mid \vec{\Omega}(\vec{k}) \mid^2 \rangle$ [123]. This quantity, together with the correlation time of the random angular diffusion of spin precession vector τ_Ω, are the relevant variables in the D'yakonov-Perel's formula

$$\tau = \frac{1}{\langle \mid \vec{\Omega}(\vec{k}) \mid^2 \rangle \tau_\Omega} \ . \tag{17}$$

Where, $1/\tau_\Omega = 1/\tau_p + 1/\tau_p^{'}$, obtained by using Matthiessen's rule. Here, τ_p is the momentum relaxation time and $\tau_p^{'}$, the momentum redistribution time, related to the electron-electron interaction mechanism.

4.1. Monte Carlo approach and Noise modelling

The conduction bands of GaAs are represented by the Γ-valley and four equivalent L-valleys. The electron transport dynamics is simulated by a semi-classical Monte Carlo approach, which takes into account all the possible scattering events of the hot electrons in the medium [124]- [126]. Moreover, we also include the electron-electron (e-e) scattering by exploiting the screened Coulomb potential and the Born's approximation. The e-e scattering is handled as an interaction between only two particles, by means of the Peschke's approach [127], as improved by Moško and Mošková [128] to take into account the e-e scattering rate valid for spin-polarised gas [129]. The complete set of n-type GaAs parameters utilized in our numerical simulations is listed in Table I of Ref. [124]. In our numerical code the spin polarisation vector is taken into account and calculated for each free electron [121, 130, 131]. All

simulations are obtained in a GaAs bulk having a doping concentration n equal to 10^{16} cm^{-3} at a lattice temperature T_L=300 K. In our algorithm all donors are considered ionised and the free electron concentration is set equal to the doping concentration. In order to collect spin statistics we simulate an ensemble of $5 \cdot 10^4$ electrons and we compute all physical quantities after a transient time long enough to get the steady-state transport regime. The spin depolarization study starts with all the carriers at the injection plane being in the Γ valley, initially polarised ($S(0) = 1$) along the $\hat{x}$-axis of the crystal. The spin lifetime τ is calculated as the time corresponding to a reduction of the initial polarisation by a factor $1/e$. Our numerical outcomes provides spin lifetimes in good agreement with those calculated in a recent theoretical paper [120] and with the experimental results reported in Ref. [132].

In our numerical calculations the GaAs sample is driven by a fluctuating electric field $F(t) = F_0 + \eta(t)$, where F_0 is the strength of the deterministic field and $\eta(t)$ is the random contribution due to the noise external source. Here we consider two different kinds of random fluctuations: a Gaussian correlated (GC) noise source and a dichotomous Markov (DM) noise source.

Gaussian correlated noise is modelled as an Ornstein-Uhlenbeck (OU) process, which obeys the following stochastic differential equation [133]

$$\frac{d\eta(t)}{\mathrm{d}t} = -\frac{\eta(t)}{\tau_c} + \sqrt{\frac{2D}{\tau_c}}\xi(t) \tag{18}$$

where τ_c and D are the correlation time and the intensity of the noise component, respectively. The autocorrelation function of the OU process is $\langle \eta(t)\eta(t') \rangle = D \exp(-|t - t'|/\tau_c)$, and $\xi(t)$ is a Gaussian white noise with zero mean $\langle \xi(t) \rangle = 0$ and $\langle \xi(t)\xi(t') \rangle = \delta(t - t')$.

The symmetric dichotomous Markov (DM) noise is generated by a random process characterized by a stochastically switching between only two discrete values [134, 135]

$$\eta(t) \in \{-\Delta, \Delta\}. \tag{19}$$

Thus, we have zero mean

$$\langle \eta(t) \rangle = 0, \tag{20}$$

and correlation function

$$\langle \eta(t)\eta(t') \rangle = \Delta^2 \exp\left(-\frac{\mid t - t' \mid}{\tau_D}\right), \tag{21}$$

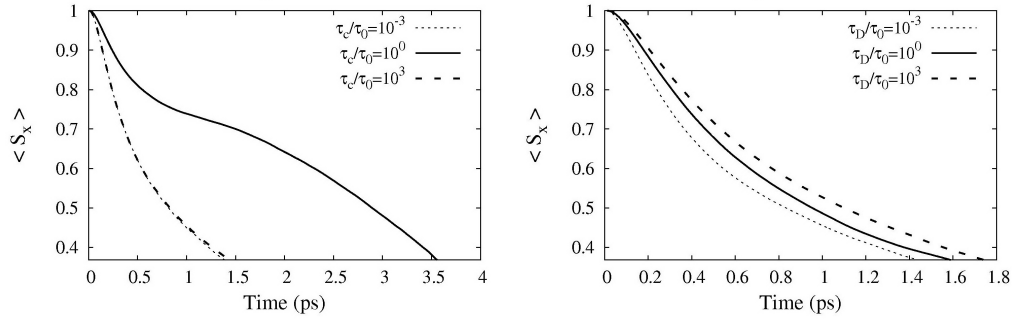

Figure 8: Spin polarisation $< S_x >$ as a function of time at three different values of the normalised correlation time τ_c/τ_0 (left panel) or τ_D/τ_0 (right panel), namely (dotted line) 10^{-3}, (solid line) 10^0 and (dashed line) 10^3. The other parameter values are: $F_0 = 6$ kV/cm, τ_0 =1.40 ps; for the Gaussian correlated noise (left) $D^{1/2} = 2.4$ kV/cm; for the dichotomous noise (right) $\Delta = 1.2$ kV/cm.

where τ_D is the correlation time of the noise and it is related to the inverse of the mean frequency of transition from $\pm\Delta$ to $\mp\Delta$, respectively [134, 135]. In our simulations, we set $\eta(0) = Z$ as initial condition, where Z is a random variable which can assume only the values Δ and $-\Delta$ with the same probability ($P = 0.5$). In this work only fluctuations of equal amplitude, easily generable by means of electronic circuits, have been taken into account in order to make more manageable the effects of the DM noise.

4.2. Numerical results and discussion

In order to investigate the effects due to the addition of external random fluctuations on the depolarisation process of the electron spin, we carried out 500 diverse noise histories for each strength of the deterministic applied field and estimated the mean value and the standard deviation of the spin relaxation times. Different findings are found, depending on whether the deterministic field F_0 is lower or higher than the Gunn field ($F_G \approx 3.25$ kV/cm), that is the minimum value of electric field that the electrons need to move in L-valleys. In panels of Figure 8, we show a single Monte Carlo realisation of the electron spin average polarisation $< S_x >$ (averaged over the electron ensemble) as a function of time. The fluctuating external field is characterised by a deterministic component with amplitude $F_0 = 6$ kV/cm and a random GC component of amplitude $D^{1/2} = 2.4$ kV/cm (left panel) or a DM random component of amplitude $\Delta = 1.2$ kV/cm (right panel), for three different values of the normalised noise correlation time τ_c/τ_0 or

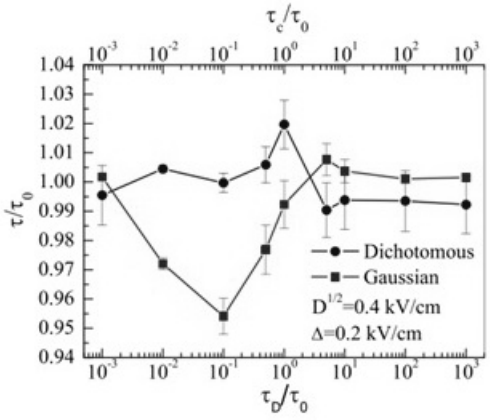

Figure 9: Normalised electron spin relaxation time τ/τ_0 as a function of the normalised correlation time τ_c/τ_0 of the GC noise or τ_D/τ_0) of the DM noise, respectively. The values of the other parameters are: $n = 10^{16}$ cm^{-3}, T_L=300 K, $F_0 = 1$ kV/cm, $D^{1/2} = 0.4$ kV/cm, $\Delta = 0.2$ kV/cm, and $\tau_0 = 42.8$ ps.

τ_D/τ_0, respectively. Here, $\tau_0 = 1.40\ ps$ is the spin relaxation time obtained when only the deterministic field F_0 is applied. The spin relaxation process is significantly influenced by the external GC fluctuation component only for values of the noise correlation time comparable to τ_0 ($\tau_c \geq \tau_0$), where the electron spin lifetime is considerably enhanced. In the case of the DM random component, when $\tau_D \ll \tau_0$, the spin dephasing process is practically not affected by the fluctuations of the electric field, which have a negligible memory (τ_D) with respect to the characteristic time τ_0 of the system, making the dephasing process quasi-deterministic. The spin relaxation process begins to be influenced by the fluctuating field only for values of the noise correlation time comparable with τ_0 ($\tau_D \geq \tau_0$).

In Fig. 9, we show the normalised electron spin lifetime τ/τ_0 as a function of the normalised noise correlation time, both for GC and DM noise, with $F_0 = 1$ kV/cm, $\Delta = 0.2$ kV/cm and $D^{1/2} = 0.4$ kV/cm. Since the amplitude of the applied electric field is not enough to allow the electrons to move in higher energy valleys ($F_0 < F_G$), independently on the noise mean switching time, the DM noise has no effect on the spin relaxation process (see circles). However, a faster spin depolarisation, with a shorter spin lifetime (up to 5%), is found if the fluctuating contribution is Gaussian correlated (see squares). In this case, the reduction strongly depends on the noise correlation time.

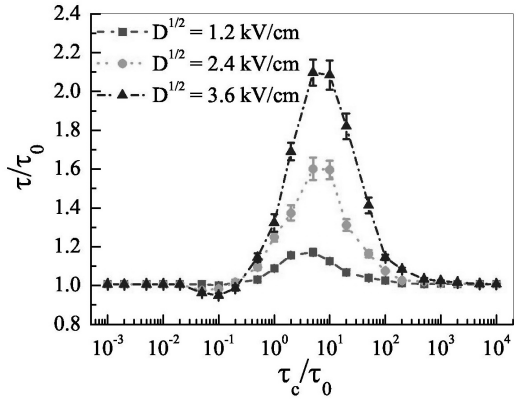

Figure 10: Results for Gaussian correlated noise: normalised electron spin relaxation time τ/τ_0 as a function of the normalised noise correlation time τ_c/τ_0, for three different values of noise amplitude, namely $D^{1/2} = 1.2, 2.4, 3.6$ kV/cm. The values of the other parameters are: $n = 10^{16}$ cm^{-3}, T_L=300 K, $F_0 = 6$ kV/cm and $\tau_0 = 1.40$ ps.

The dependence of the normalised spin relaxation time τ/τ_0 on the normalised noise correlation time τ_c/τ_0, in the case of a driving electric field fluctuating for the presence of an external source of GC noise, is shown in Fig. 10, for three different values of the noise intensity. A detailed analysis of these data highlights the presence of a nonmonotonic behaviour characterised by a slight minimum at $\tau_c/\tau_0 \sim 10^{-1}$ and a more evident maximum for a value of the noise correlation time of about 10 τ_0. Our results show that the addition of a Gaussian correlated noise, with τ_c in the range $(1 \div 100)\tau_0$, causes an enhancement of the value of the spin relaxation time τ which may increase up to ~ 2.1 τ_0 depending on the value of the noise intensity D. For very low and very high values of τ_c, the time τ remains close to τ_0. In the presence of Gaussian correlated fluctuations, the electron ensemble experiences an effective electric field that can be higher or lower than the deterministic one, depending on the value of the noise correlation time, the characteristic memory time of the fluctuations. This affects the electron transport in the semiconductor in such a way that an enhancement or a reduction of the electron spin lifetime, occupation percentage and hot-electron temperature can be obtained [56]. The occurrence of these circumstances depends not only on the ratio between the value of the memory time of the GC noise and the characteristic relaxation time of the spin system, but also on its ratio with both the momentum relaxation time and the momentum redistribution time

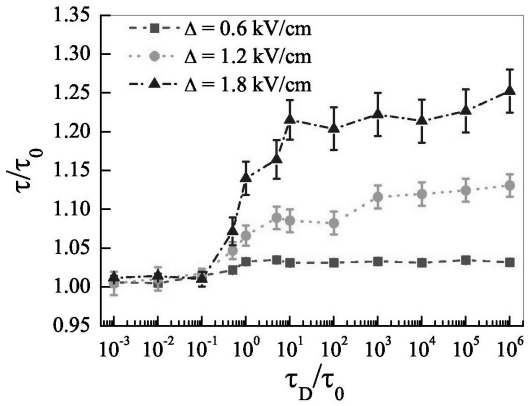

Figure 11: Results for dichotomous Markov noise: normalised electron spin relaxation time τ/τ_0 as a function of the normalised noise correlation time τ_D/τ_0, for three different values of noise amplitude, namely $\Delta = 0.6, 1.2, 1.8$ kV/cm. The values of the other parameters are: $n = 10^{16}$ cm^{-3}, T_L=300 K, $F_0 = 6$ kV/cm and $\tau_0 = 1.40$ ps.

(characteristic of the electron-electron interaction). Thus, if the GC noise becomes "resonant" with one of these characteristic times of the system, it can give rise to a constructive or destructive interference, and produce significant changes on the electron dynamics [56]. The influence of different time scales on the spin polarised transport in GaAs and other semiconductor materials needs deeper analysis and will be subject of further investigations.

In Fig. 11, we show the normalised electron spin relaxation time τ/τ_0 as a function of the normalised correlation time τ_D/τ_0, for different values of the DM noise amplitude Δ. For the lowest noise amplitude $\Delta = 0.6$ kV/cm, the electron spin relaxation time is almost constant ($\tau/\tau_0 \sim 1$). For values of the noise correlation time $\tau_D \leq 10^{-1}\tau_0$, the value of τ is always close to τ_0, even at higher values of Δ. On the contrary, when the noise amplitude increases and $\tau_D > \tau_0$, the value of the spin relaxation time τ can increase up to 1.25 τ_0. For $\tau_D > 10$ τ_0, the electron spin lifetime remains approximately constant. This positive effect monotonically increases with the amplitude of the DM noise. A threshold effect is observed, in which an enhancement of the electron spin lifetime can be maintained for several orders of magnitude of the DM mean switching time, starting from a value equal to 10 times the relaxation characteristic time τ_0 of the spin system in the absence of noise. A simple argument to explain the numerical results found in the presence of an external source of DM noise has been extensively discussed in Ref. [56].

5. Conclusions

The investigation of three noise induced effects in the transient dynamics of out of equilibrium condensed matter systems has been reviewed. Specifically, we analyzed the noise enhanced stability and the stochastic resonant activation phenomena in the nonlinear relaxation of (i) a long JJ in the presence of non-Gaussian noise source, (ii) a short grapheme based JJ, and (iii) the noise-induced coherence of electron spin in a n-doped GaAs semiconductor crystal.

(i) In long current-biased Josephson junctions, the effects of non-Gaussian noise sources on the mean switching times (MST), using different Lévy distributions, have been presented. Specifically, we have shown how the out of equilibrium dynamics of long JJs is affected by Lévy flights and noise-induced solitons. In particular, in the behaviour of the MST, we observed noise induced phenomena such as *stochastic resonant activation* (SRA) and *noise enhanced stability* (NES), with different characteristics depending on both the bias current and the length of the superconducting device. The analysis of the MST as a function of the junction length revealed that the *soliton dynamics* plays a crucial role in the switching dynamics from the superconducting to resistive state. The MST from one of the metastable states of the potential profile encodes information on the non-Gaussian background noise. Therefore, the statistical analysis of the switching times of JJs can be used to analyse weak signals in the presence of an unknown non-Gaussian background noise.

(ii) The short JJ studied in this work is composed by two superconducting elements suspended on a graphene layer. As a consequence, the critical current of a graphene-based JJ deviates from the conventional sinusoidal behaviour. A comparison between the mean first passage times calculated for normal and graphene-based devices, changing the initial bias current value, is presented. Noise induced behaviours have been observed, that is RA and NES effects, with characteristics depending on the kind of junction taken into account. The nonmonotonic behaviours of the superconducting lifetime as a function of the driving frequency and noise intensity could give rise to a new generation of graphene-based JJs. Our results show that, by controlling the escape process from the metastable state, we can improve the performance of short and long JJ devices and reveal non-Gaussian background noise present in input unknown signals.

(iii) We have also analysed the influence of two different noise sources on

the electron spin relaxation process in n-doped GaAs semiconductor crystals. Our findings show that in the case of Gaussian correlated fluctuations, the spin relaxation time has a nonomonotonic behaviour, with a maximum. In particular, when the noise memory time is comparable with one of the characteristic times of the electron dynamics, a constructive or destructive interference effect occurs giving rise to an enhancement or a reduction of the spin relaxation time. With the addition of DM random fluctuations to a static driving electric field, whose amplitude is greater than the Gunn threshold, it is possible to enhance the spin lifetime up to 25% of its value in the absence of external noise. This enhancement, which increases with the amplitude of the external fluctuations, is observed for noise correlation times comparable or greater than the spin lifetime obtained with the only deterministic applied field. The enhancement of the electron spin lifetime in GaAs crystals strongly depends on the correlation time and amplitude of the external Gaussian correlated noise. In particular, we have found that the benefits of the dichotomous noise consist in a threshold effect, in which the increase of the electron spin lifetime is obtained in a wide range of noise correlation times, while in the presence of a Gaussian correlated noise, the enhancement is greater, but is obtainable only in a limited range of correlation times. In conclusion, random fluctuations of the electric driving field, due to different noise sources, can play a relevant role on controlling and tuning the coherence of spin-relaxation processes. In this view, by using appropriate characteristic times for the noise sources, it is possible to select the most favourable condition for the transmission of information by electron spin.

The noise can stabilize a metastable state in fluctuating driven JJ systems, by increasing its lifetime. Moreover, the noise can enhance the spin lifetime in a spintronic system by increasing the coherence of the spin relaxation process from an initial metastable state. The results presented in this paper are general enough to be extended to out of equilibrium condensed matter and complex biological systems characterized by the presence of metastable states.

6. Acknowledgements

This work was partially supported by Ministry of Education, University, and Research of Italian Government (MIUR) through Grant No. PON02 00355 3391233, ENERGETIC.

References

[1] G. Wendin, V. Shumeiko, Quantum bits with Josephson junctions (review article), Low Temp. Phys.+ 33 (9) (2007) 724–744.

[2] J. H. Kim, R. P. Dhungana, K.-S. Park, Decoherence in Josephson vortex quantum bits: Long-Josephson-junction approach to a two-state system, Phys. Rev. B 73 (21) (2006) 214506.

[3] A. Zorin, E. Tolkacheva, M. Khabipov, F.-I. Buchholz, J. Niemeyer, Dynamics of Josephson junctions and single-flux-quantum networks with superconductor–insulator–normal-metal junction shunts, Phys. Rev. B 74 (1) (2006) 014508.

[4] A. Berkley, H. Xu, M. Gubrud, R. Ramos, J. Anderson, C. Lobb, F. Wellstood, Decoherence in a Josephson-junction qubit, Phys.Rev. B 68 (6) (2003) 060502.

[5] C. Wu, Y. Chou, W. Kuo, J. Chen, L. Wang, J. Chen, K. Chen, U. Sou, H. Yang, J. Jeng, Fabrication and characterisation of high-tc yba2cu3o7-x nanosquids made by focused ion beam milling, Nanotechnology 19 (31) (2008) 315304.

[6] E. Levenson-Falk, R. Vijay, N. Antler, I. Siddiqi, A dispersive nanosquid magnetometer for ultra-low noise, high bandwidth flux detection, Supercond. Sci. Tech. 26 (5) (2013) 055015.

[7] H. Grabert, Theory of a Josephson junction detector of non-Gaussian noise, Phys. Rev. B 77 (20) (2008) 205315.

[8] D. Urban, H. Grabert, Feedback and rate asymmetry of the Josephson junction noise detector, Phys. Rev. B 79 (11) (2009) 113102.

[9] G. Filatrella, V. Pierro, Detection of noise-corrupted sinusoidal signals with Josephson junctions, Phys. Rev. E 82 (4) (2010) 046712.

[10] P. Addesso, G. Filatrella, V. Pierro, Characterisation of escape times of Josephson junctions for signal detection, Phys. Rev. E 85 (1) (2012) 016708.

[11] P. Reimann, C. Van den Broeck, H. Linke, P. Hänggi, J. Rubi, A. Pérez-Madrid, Giant acceleration of free diffusion by use of tilted periodic potentials, Phys. Rev. Lett. 87 (1) (2001) 010602.

[12] A. A. Dubkov, B. Spagnolo, Acceleration of diffusion in randomly switching potential with supersymmetry, Phys. Rev. E 72 (4) (2005) 041104.

[13] B. Huard, H. Pothier, N. O. Birge, D. Esteve, X. Waintal, J. Ankerhold, Josephson junctions as detectors for non-Gaussian noise, Ann. Phys-Berlin 16 (10-11) (2007) 736–750.

[14] T. Novotnỳ, Josephson junctions as threshold detectors of full counting statistics: open issues, J. Stat. Mech.-Theory E. 2009 (01) (2009) P01050.

[15] Q. Le Masne, H. Pothier, N. O. Birge, C. Urbina, D. Esteve, Asymmetric noise probed with a Josephson junction, Phys. Rev. Lett. 102 (6) (2009) 067002.

[16] L. Billings, M. I. Dykman, I. B. Schwartz, Thermally activated switching in the presence of non-Gaussian noise, Phys. Rev. E 78 (5) (2008) 051122.

[17] J. Peltonen, A. Timofeev, M. Meschke, T. Heikkilä, J. Pekola, Detecting non-Gaussian current fluctuations using a Josephson threshold detector, Physica E: Low-dimensional Systems and Nanostructures 40 (1) (2007) 111–122.

[18] J. Tobiska, Y. V. Nazarov, Josephson junctions as threshold detectors for full counting statistics, Phys. Rev. Lett. 93 (10) (2004) 106801.

[19] J. Ankerhold, Detecting charge noise with a Josephson junction: A problem of thermal escape in presence of non-Gaussian fluctuations, Phys. Rev. Lett. 98 (3) (2007) 036601.

[20] E. V. Sukhorukov, A. N. Jordan, Stochastic dynamics of a Josephson junction threshold detector, Phys. Rev. Lett. 98 (13) (2007) 136803.

[21] M. Köpke, J. Ankerhold, Linear dynamics subject to thermal fluctuations and non-Gaussian noise: from classical to quantum, New J. Phys. 5 (4) (2013) 043013.

[22] C. Guarcello, D. Valenti, G. Augello, B. Spagnolo, The role of non-Gaussian sources in the transient dynamics of long Josephson junctions, Acta Phys. Pol. B 44 (5) (2013) 997–1005.

[23] D. Valenti, C. Guarcello, B. Spagnolo, Switching times in long-overlap Josephson junctions subject to thermal fluctuations and non-Gaussian noise sources, Phys. Rev. B 89 (21) (2014) 214510.

[24] E. Montroll, M. Shlesinger, Nonequilibrium Phenomena II: From Stochastics to Hydrodynamics, edited by J. L. Lebowitz and E. W. Montroll, North-Holland, Amsterdam, 1984.

[25] M. F. Shlesinger, G. M. Zaslavsky, U. Frisch, Lévy Flights and Related Topics in Physics, Springer-Verlag, Berlin, 1955.

[26] B. Dybiec, E. Gudowska-Nowak, Resonant activation in the presence of nonequilibrated baths, Phys. Rev. E 69 (1) (2004) 016105.

[27] M. R. Souryal, E. G. Larsson, B. Peric, B. R. Vojcic, Soft-decision metrics for coded orthogonal signaling in symmetric alpha-stable noise, IEEE T. Signal Process. 56 (1) (2008) 266–273.

[28] G.-H. Lee, D. Jeong, J.-H. Choi, Y.-J. Doh, H.-J. Lee, Electrically tunable macroscopic quantum tunnelling in a graphene-based Josephson junction, Phys. Rev. Lett. 107 (14) (2011) 146605.

[29] J.-H. Choi, G.-H. Lee, S. Park, D. Jeong, J.-O. Lee, H.-S. Sim, Y.-J. Doh, H.-J. Lee, Complete gate control of supercurrent in graphene p–n junctions, Nature Communications 4 (2013), 2525, 1–10.

[30] M. Titov, C. W. Beenakker, Josephson effect in ballistic graphene, Phys. Rev. B 74 (4) (2006) 041401.

[31] J. G. Lambert, S. A. Carabello, R. C. Ramos, Analysis of possible quantum metastable states in ballistic graphene-based Josephson junctions, IEEE T. Appl. Supercon. 21 (3) (2011) 734–737.

[32] X. Du, I. Skachko, E. Y. Andrei, Josephson current and multiple Andreev reflections in graphene sns junctions, Phys. Rev. B 77 (18) (2008) 184507.

[33] F. Miao, W. Bao, H. Zhang, C. N. Lau, Premature switching in graphene Josephson transistors, Solid State Commun. 149 (27) (2009) 1046–1049.

[34] D. Jeong, J.-H. Choi, G.-H. Lee, S. Jo, Y.-J. Doh, H.-J. Lee, Observation of supercurrent in pbin-graphene-pbin Josephson junction, Phys. Rev. B 83 (9) (2011) 094503.

[35] U. Coskun, M. Brenner, T. Hymel, V. Vakaryuk, A. Levchenko, A. Bezryadin, Distribution of supercurrent switching in graphene under the proximity effect, Phys. Rev. Lett. 108 (9) (2012) 097003.

[36] N. Mizuno, B. Nielsen, X. Du, Ballistic-like supercurrent in suspended graphene Josephson weak links, Nature Communications 4 (2013) 2716, 1–6.

[37] E. L. Pankratov, B. Spagnolo, Optimization of impurity profile for p-n junction in heterostructures, Eur. Phys. J. B 46 (2005) 15–19.

[38] F. Cadiz, P. Barate, D. Paget, D. Grebenkov, J. P. Korb, A. C. H. Rowe, T. Amand, S. Arscott, E. Peytavit, All optical method for investigation of spin and charge transport in semiconductors: Combination of spatially and time-resolved luminescence, J. Appl. Phys. 116 (2014), 023711.

[39] S. A. Wolf, D. D Awschalom, R. A Buhrman, J. M. Daughton, S. Von Molnár, M. L. Roukes, A. Y. Chtchelkanova, D. M. Treger, Spintronics: A Spin-Based Electronics Vision for the Future, Science 294 (2001) 1488–1495.

[40] I. Žutić, J. Fabian, S. Das Sarma, Spintronics: Fundamentals and applications, Rev. Mod. Phys. 76 (2004) 323–410.

[41] J. Fabian, A. Matos-Abiague, C. Ertler, P. Stano, I. Žutić, Semiconductor Spintronics, Acta Phys. Slovaca 57 (2007) 565–907.

[42] B. Behin-Aein, D. Datta, S. Salahuddin, S. Datta, Proposal for an all-spin logic device with built-in memory, Nat. Nanotech. 5 (2010) 266–270.

[43] F. Pulizzi, Spintronics, Nat. Mater. 11 (2012) 367.

[44] S. Salahuddin, Solid-state physics: A new spin on spintronics, Nature 494 (2013) 43–44.

[45] M. A. Lodato, D. Persano Adorno, N. Pizzolato, B. Spagnolo, External Noise E?ects in Silicon MOS Inversion Layer, Acta Phys.Pol. B 44 (2013) 1163-1172.

[46] R. Mantegna, B. Spagnolo, Noise enhanced stability in an unstable system, Phys. Rev. Lett. 76 (1996) 563–566.

[47] N. Agudov, B. Spagnolo, Noise-enhanced stability of periodically driven metastable states, Phys. Rev. E 64 (3) (2001) 035102.

[48] A. A. Dubkov, N. V. Agudov, B. Spagnolo, Noise-enhanced stability in fluctuating metastable states, Phys. Rev. E 69 (6) (2004) 061103.

[49] D. Persano Adorno, N. Pizzolato, B. Spagnolo, External Noise Effects on the Electron Velocity Fluctuations in Semiconductors, Acta Phys. Pol. A 113 (200) 985–988.

[50] D. Persano Adorno, N. Pizzolato, B. Spagnolo, Noise influence on electron dynamics in semiconductors driven by a periodic electric field, J. Stat. Mech.-Theory E. (2009) P01039.

[51] D. Persano Adorno, N. Pizzolato, D. Valenti, B. Spagnolo, External noise effects in doped semiconductors operating under sub-THz signals, Rep. Math. Phys. 70 (2012) 171–179.

[52] V. K. Dugaev, M. Inglot, E. Ya. Sherman, J. Barnas, Spin Hall effect and spin current generation in two-dimensional systems with random Rashba spin-orbit coupling, J. Magn. Magn. Mater. 324 (2012) 3573–3575.

[53] P. Agnihotri, S. Bandyopadhyay, Spin dynamics and spin noise in the presence of randomly varying spin-orbit interaction in a semiconductor quantum wire, J. Phys.-Condens. Mat. 24 (2012) 215302.

[54] S. Spezia, D. Persano Adorno, N. Pizzolato, B. Spagnolo, New insights into electron spin dynamics in the presence of correlated noise, J. Phys.-Condens. Mat. 24 (2012) 052204.

[55] S. Spezia, D. Persano Adorno, N. Pizzolato, B. Spagnolo, Effect of a Fluctuating Electric Field on Electron Spin Dephasing Time in III-V Semiconductors, Acta Phys. Pol. B 43 (2012) 1191–1201.

[56] S. Spezia, D. Persano Adorno, N. Pizzolato, B. Spagnolo, Enhancement of electron spin lifetime in GaAs crystals: the benefits of dichotomous noise, Europhys. Lett. 104 (2013) 47011.

[57] A. Barone, G. Paterno, Physics and applications of the Josephson effect, Wiley, 1982.

[58] K. Likharev, Dynamics of Josephson Junctions and Circuits, Gordon & Breach, New York, 1986.

[59] M. Buttikcr, R. Landauer, Nucleation theory of overdamped soliton motion, Phys. Rev. A 23 (1981), 1397–1410.

[60] F. Marchesoni, Solitons in a random field of force: A Langevin equation approach, Phys. Lett. A 115 (1986), 29–32.

[61] P. Hänggi, F. Marchesoni, P. Sodano, Nucleation of Thermal Sine-Gordon Solitons: Effect of Many-Body Interactions, Phys. Rev. Lett. 60 (1988), 2563–2566.

[62] F. Marchesoni, Thermal Ratchets in 1 + 1 Dimensions, Phys. Rev. Lett. 77 (1996), 2364–2367.

[63] A. V. Ustinov, Solitons in Josephson junctions Physica D 123 (1998) 315–329.

[64] Yuri S. Kivshari, Barry Luther-Davies Dark Optical Solitons: Physics and Applications Physics Reports 298 (1998) 81–197.

[65] W. A. Woyczynski, Lévy Processes: Theory and Applications, Birkhauser, Boston, 2001.

[66] J. Bertoin, Lévy Processes, Cambridge University Press, Cambridge, 1996.

[67] K. Sato, Lévy processes and infinitely divisible distributions, Cambridge University Press, Cambridge, UK, 1999.

[68] B. V. Gnedenko, A. N. Kolmogorov, Limit distributions for sums of independent random variables, Addison-Wesley Publishing Company, Inc., Cambridge, Massachusetts, 1954.

[69] B. De Finetti, Theory of Probability: A critical introductory treatment, John Wiley & Sons, New York, 1974.

[70] A. Khintchine, P. Lévy, Sur les lois stables, C. R. Acad. Sci. Paris 202.

[71] A. Y. Khintchine, Limit Distributions for the Sum of Independent Random Variables, O.N.T.I, Moscow (in Russian), 1938.

[72] W. Feller, An introduction to probability theory and its applications, Vol. 2, John Wiley & Sons, 2008.

[73] R. Weron, On the Chambers-Mallows-Stuck method for simulating skewed stable random variables, Stat. & Probabil. Lett. 28 (2) (1996) 165–171.

[74] J. M. Chambers, C. L. Mallows, B. Stuck, A method for simulating stable random variables, J. Am. Stat. Assoc. 71 (354) (1976) 340–344.

[75] K. Binder, Time-Dependent Ginzburg-Landau Theory of Nonequilibrium Relaxation, Phys. Rev. B 8 (1973) 3423–3438.

[76] N. V. Agoudov, A. N. Malakhov, Nonstationary diffusion through arbitrary piecewise-linear potential profile. Exact solution and time characteristics Radiophys. Quantum El. 36 (2) (1993) 97–109.

[77] A. N. Malakhov, Time scales of overdamped nonlinear Brownian motion in arbitrary potential profiles, Chaos 7(3) (1997) 488–504.

[78] A. A. Dubkov, A. N. Malakhov, A. I. Saichev, Correlation time and structure of the correlation function of nonlinear equilibrium Brownian motion in arbitrary-shaped potential wells, Radiophys. Quantum El. 43(4) (2000) 335–346.

[79] A. N. Malakhov, A. L. Pankratov, Evolution times of probability distributions and averages–exact solutions of the Kramers'problem, Adv. Chem. Phys. 121 (2002) 357–438.

[80] K. Fedorov, A. L. Pankratov, B. Spagnolo, Influence of length on the noise delayed switching of long Josephson junctions, Int. J. Bifurcat. Chaos 18 (09) (2008) 2857–2862.

[81] C. R. Doering, J. C. Gadoua, Resonant activation over a fluctuating barrier, Phys. Rev. Lett. 69 (16) (1992) 2318–2321.

[82] R. N. Mantegna, B. Spagnolo, Experimental investigation of resonant activation, Phys. Rev. Lett. 84 (14) (2000) 3025–3028.

[83] R. Mantegna, B. Spagnolo, Numerical simulation of resonant activation in a fluctuating metastable model system, J. Phys. IV 8 (PR6) (1998) Pr6-247–251.

[84] P. Pechukas, P. Hänggi, Rates of activated processes with fluctuating barriers, Phys. Rev. Lett. 73 (20) (1994) 2772–2775.

[85] M. Marchi, F. Marchesoni, L. Gammaitoni, E. Menichella-Saetta, S. Santucci, Resonant activation in a bistable system, Phys. Rev. E 54 (4) (1996) 3479–3487.

[86] B. Dybiec, E. Gudowska-Nowak, Lévy stable noise-induced transitions: Stochastic resonance, resonant activation and dynamic hysteresis, J. Stat. Mech.-Theory E. (2009) P05004.

[87] S. Miyamoto, K. Nishiguchi, Y. Ono, K. M. Itoh, A. Fujiwara, Resonant escape over an oscillating barrier in a single-electron ratchet transfer, Phys. Rev. B 82 (3) (2010) 033303.

[88] N. Pizzolato, A. Fiasconaro, D. Persano Adorno, B. Spagnolo, Resonant activation in polymer translocation: new insights into the escape dynamics of molecules driven by an oscillating field, Phys. Biol. 7 (2010) 034001.

[89] Y. Hasegawa, M. Arita, Escape process and stochastic resonance under noise intensity fluctuation, Phys. Lett. A 375 (39) (2011) 3450–3458.

[90] A. Fiasconaro, B. Spagnolo, Resonant activation in piecewise linear asymmetric potentials, Phys. Rev. E 83 (4) (2011) 041122.

[91] N. Pizzolato, A. Fiasconaro, D. Persano Adorno, B. Spagnolo, Translocation dynamics of a short polymer driven by an oscillating force, J. Chem. Phys. 138 (2013), 054902.

[92] G. Augello, D. Valenti, B. Spagnolo, Non-gaussian noise effects in the dynamics of a short overdamped josephson junction, Eur. Phys. J. B 78 (2) (2010) 225–234.

[93] C. Pan, X. Tan, Y. Yu, G. Sun, L. Kang, W. Xu, J. Chen, P. Wu, Resonant activation through effective temperature oscillation in a Josephson tunnel junction, Phys. Rev. E 79 (3) (2009) 030104.

[94] M. H. Devoret, J. M. Martinis, D. Esteve, J. Clarke, Resonant activation from the zero-voltage state of a current-biased josephson junction, Phys. Rev. Lett. 53 (13) (1984) 1260–1263.

[95] M. H. Devoret, J. M. Martinis, J. Clarke, Measurements of macroscopic quantum tunneling out of the zero-voltage state of a current-biased Josephson junction, Phys. Rev. Lett. 55 (18) (1985) 1908–1911.

[96] J. M. Martinis, M. H. Devoret, J. Clarke, Experimental tests for the quantum behavior of a macroscopic degree of freedom: The phase difference across a Josephson junction, Phys. Rev. B 35 (10) (1987) 4682–4698.

[97] R. N. Mantegna, B. Spagnolo, Probability distribution of the Residence Times in Periodically Fluctuating Metastable Systems, Int. J. Bifurcat. Chaos 8(4) (1998) 783–790.

[98] N. V. Agudov, A. A. Dubkov, B. Spagnolo, Escape from a metastable state with fluctuating barrier, Physica A 325 (2003) 144-151.

[99] A. Fiasconaro, D. Valenti, B. Spagnolo, Role of the initial conditions on the enhancement of the escape time in static and fluctuating potentials, Physica A 325 (2003) 144–151.

[100] B. Spagnolo, A. A. Dubkov, and N. V. Agudov, Enhancement of stability in randomly switching potential with metastable state, Eur. Phys. J. B 40 (2004) 273–281.

[101] B. Spagnolo, N. Agudov, A. Dubkov, Noise enhanced stability, Acta Phys. Pol. B 35 (4) (2004) 1419–1436.

[102] P. D'Odorico, F. Laio, L. Ridolfi, Noise-induced stability in dryland plant ecosystems, P. Natl. Acad. Sci. USA 102 (31) (2005) 10819–10822.

[103] A. Fiasconaro, B. Spagnolo, S. Boccaletti, Signatures of noise-enhanced stability in metastable states, Phys. Rev. E 72 (6) (2005) 061110.

[104] A. Fiasconaro, B. Spagnolo, A. Ochab-Marcinek, E. Gudowska-Nowak, Co-occurrence of resonant activation and noise-enhanced stability in a model of cancer growth in the presence of immune response, Phys. Rev. E 74 (2006) 041904(10).

[105] P. I. Hurtado, J. Marro, P. Garrido, Metastability, nucleation, and noise-enhanced stabilization out of equilibrium, Phys. Rev. E 74 (5) (2006) 050101.

[106] B. Spagnolo, A. Dubkov, A. Pankratov, E. Pankratova, A. Fiasconaro, A. Ochab-Marcinek, Lifetime of metastable states and suppression of noise in interdisciplinary physical models, Acta Phys. Pol. B 38 (5) (2007) 1925–1950.

[107] G. Bonanno, D. Valenti, B. Spagnolo, Mean escape time in a system with stochastic volatility, Phys. Rev. E 75 (2007) 016106(8).

[108] R. Mankin, E. Soika, A. Sauga, A. Ainsaar, Thermally enhanced stability in fluctuating bistable potentials, Phys. Rev. E 77 (5) (2008) 051113.

[109] A. Fiasconaro, A. Ochab-Marcinek, B. Spagnolo, E. Gudowska-Nowak, Monitoring noise-resonant effects in cancer growth influenced by spontaneous fluctuations and periodic treatment, Eur. Phys. J. B 65 (2008) 435–442.

[110] M. Yoshimoto, H. Shirahama, S. Kurosawa, Noise-induced order in the chaos of the Belousov–Zhabotinsky reaction, J. Chem. Phys. 129 (1) (2008) 014508.

[111] A. Fiasconaro, B. Spagnolo, Stability measures in metastable states with Gaussian colored noise, Phys. Rev. E 80 (4) (2009) 041110.

[112] M. Trapanese, Noise enhanced stability in magnetic systems, J. Appl. Phys. 105 (7) (2009) 07D313.

[113] A. Fiasconaro, J. J. Mazo, B. Spagnolo, Noise-induced enhancement of stability in a metastable system with damping, Phys. Rev. E 82 (4) (2010) 041120.

[114] J.-h. Li, J. Łuczka, Thermal-inertial ratchet effects: Negative mobility, resonant activation, noise-enhanced stability, and noise-weakened stability, Phys. Rev. E 82 (4) (2010) 041104.

[115] A. A. Smirnov, A. L. Pankratov, Influence of the size of uniaxial magnetic nanoparticle on the reliability of high-speed switching, Phys. Rev. B 82 (13) (2010) 132405.

[116] A. Shit, S. Chattopadhyay, J. R. Chaudhuri, Quantum Stochastic Dynamics in the Presence of a Time-Periodic Rapidly Oscillating Potential: Nonadiabatic Escape Rate J. Phys. Chem. A 117 (2013) 8576-8590.

[117] T. Yang, C. Zhang, Q. Han, C.-H. Zeng, H. Wang, D. Tian, F. Long, Noises- and delay-enhanced stability in a bistable dynamical system describing chemical reaction, Eur. Phys. J. B 87 (2014) 136.

[118] M. I. D'yakonov, V. I.Perel, Possibility of Orienting Electron Spins with Current, JETP Lett. 13 (1971) 467–469.

[119] K. L. Litvinenko, M. A. Leontiadou, J. Li, S. K. Clowes, M. T. Emeny, T. Ashley, C. R. Pidgeon, L. F. Cohen, B. N. Murdin, Strong dependence of spin dynamics on the orientation of an external magnetic field for InSb and InAs, Appl. Phys. Lett. 96 (2010) 111107.

[120] H. Tong, M. W. Wu, Multivalley spin relaxation in n-type bulk GaAs in the presence of high electric fields, Phys. Rev. B 85 (2012) 075203.

[121] S. Saikin, M. Shen, M. C. Cheng, Spin dynamics in a compound semiconductor spintronic structure with a Schottky barrier, J. Phys.-Condens. Mat. 18 (2006) 1535–1544.

[122] J. Y. Fu, M. Q. Weng, M. W. Wu, Spin-orbit coupling in bulk GaAs, Physica E 40 (2008) 2890–2893.

[123] C.P. Slichter, Principles of Magnetic Resonance, edited by H.K.V. Lotsch, Springer-Verlag, Berlin, 1996 pp. 399.

[124] D. Persano Adorno, M. Zarcone, G. Ferrante, Far-infrared harmonic generation in semiconductors: A Monte Carlo simulation, Laser Phys. 10 (2000) 310–315.

[125] D. Persano Adorno, M. Zarcone, G. Ferrante, Monte Carlo simulation of harmonic generation in InP, Laser Part. Beams 19 (2001) 81–85.

[126] D. Persano Adorno, Polarization of the radiation emitted in GaAs semiconductors driven by far-infrared fields, Laser Phys. 20 (2010) 1061–1067.

[127] C. Peschke, The impact of electron-electron interaction on electron transport in GaAs at high electric fields, J. Phys.-Condens. Mat. 6 (1994) 7027–7044.

[128] M. Moško, A. Mošková, Ensemble Monte Carlo simulation of electron-electron scattering: Improvements of conventional methods, Phys. Rev. B 44 (1991) 10794–1083.

[129] A. Mošková, M. Moško, Exchange carrier-carrier scattering of photoexcited spin-polarized carriers in GaAs quantum wells: Monte Carlo study, Phys. Rev. B 49 (1994) 7443–7452.

[130] S. Spezia, D. Persano Adorno, N. Pizzolato, B. Spagnolo, Relaxation of electron spin during high-field transport in GaAs bulk, J. Stat. Mech.-Theory E. (2010) P11033.

[131] S. Spezia, D. Persano Adorno, N. Pizzolato, B. Spagnolo, Temperature dependence of spin depolarization of drifting electrons in n-type GaAs bulks, Acta Phys. Pol. B 41 (2010) 1172–1180.

[132] E. R. Viana, G. M. Ribeiro, A. G. De Oliveira, M. L. Peres, R. M. Rubinger, C. P. L. Rubinger, Antilocalization effect on photo-generated carriers in semi-insulating GaAs sample, Mater. Res.-Ibero-Am.J. 15 (2012) 530–535.

[133] C. Gardiner, Stochastic Methods: A Handbook for the Natural and Social Sciences (Springer Series in Synergetics, Springer: Complexity), fourth edition, Springer-Verlag, Berlin 2009.

[134] I. Bena, Dichotomous Markov noise: Exact results for out-of-equilibrium systems. A review, Int. J. Mod. Phys. B 20 (2006) 2825–2888.

[135] D. Barik, P. K. Ghosh, D. S. Ray, Langevin dynamics with dichotomous noise; direct simulation and applications, J. Stat. Mech.-Theory E. (2006) P03010.